AC Impedance Spectroscopy of Native DNA and M-DNA

Yi-Tao Long,*† Chen-Zhong Li,*† Heinz-Bernhard Kraatz,* and Jeremy S. Lee†
*Department of Chemistry, University of Saskatchewan, Saskatoon, SK, Canada S7N 5C9; and †Department of Biochemistry, University of Saskatchewan, Saskatoon, SK, Canada S7N 5E5

ABSTRACT Monolayers of thiol-labeled DNA duplexes of 15, 20, and 30 basepairs were assembled on gold electrodes. Electron transfer was investigated by electrochemical impedance spectroscopy with $Fe(CN)_6^{3-/4-}$ as a redox probe. The spectra, in the form of Nyquist plots, were analyzed with a modified Randles circuit which included an additional component in parallel, R_x, for the resistance through the DNA. For native B-DNA R_x and R_{ct}, the charge transfer resistance, both increase with increasing length. M-DNA was formed by the addition of Zn^{2+} at pH 8.6 and gave rise to characteristic changes in the Nyquist plots which were not observed upon addition of Mg^{2+} or at pH 7.0. R_x and R_{ct} also increased with increasing duplex length for M-DNA but both were significantly lower compared to B-DNA. Therefore, electron transfer via the metal DNA film is faster than that of the native DNA film and certain metal ions can modulate the electrochemical properties of DNA monolayers. The results are consistent with an ion-assisted long-range polaron hopping mechanism for electron transfer.

INTRODUCTION

The electronic conductivity of DNA is an important issue for the development of DNA biosensors, so-called ''DNA chips'' (Bixon et al., 1999; Schena et al., 1996; Fodor et al., 1993). The simplest form of DNA chip consists of single-stranded DNA probes attached to a surface in an array format. The target DNA is labeled with a fluorescent tag and successful hybridization to an individual probe is detected fluorometrically. Electrochemical detection, on the other hand, would have the advantage of allowing a direct readout of the signal (Takagi, 2001; Kelly et al., 1999). Electrochemical techniques include potential step chronoamperometry, DC cyclic voltammetry, and electrochemical impedance (Bard and Faulkner, 2001; Jackson and Hill, 2001; Gooding, 2002). Many electrochemical DNA sensors utilize electrochemically active DNA binding drugs such as the metal coordination complex $Ru(bpy)_3^{2+}$ (Carter and Bard, 1987; Millan et al., 1994), electroactive dyes (Hashimoto et al., 1994), quinones (Kertesz et al., 2000; Ambroise and Maiya, 2000), and methyl blue (Tani et al., 2001; Kelley et al., 1997) as the detection markers. In other cases the simple redox probe, $Fe(CN)_6^{3-/4-}$, has been used in solution (Patolsky et al., 2001). Thus a second potential advantage of these techniques is that the target DNA need not be labeled in advance. Impedance spectroscopy is of particular interest since the electronic characteristics of surface modified electrodes can be probed and the data modeled by an equivalent circuit (Macdonald, 1987). Some studies of impedance spectroscopy of DNA monolayers have been reported but detailed analysis of the electron transfer properties has not been performed (Bardea et al., 1999; Patolsky et al., 2001; Lee and Shim, 2001; Alfonta and Willner, 2001; Yan and Sadik, 2001a,b).

Electron transfer through self-assembled alkanethiol and related monolayers on metal surfaces has been intensively studied in recent years (Ulman, 1996; Colonna and Echegoyen, 2001; Kim and Kwak, 2001). The impedance of an electrode undergoing heterogeneous electron transfer through a self-assembled monolayer is usually described on the basis of the model developed by Randles (1947). The equivalent electrical circuit (Fig. 1 in *dotted box*) consists of resistive and capacitance elements. R_s is the solution resistance, R_{ct} is the charge transfer resistance, C is the double-layer capacitance, and W is the Warburg impedance due to mass transfer to the electrode. In general the Randles circuit provides a good model for the behavior of alkanethiol monolayers. Of considerable interest is the observation that monolayers of HMB (4′-hydroxy-4-mercaptobiphenyl) which contain a conjugated π-system cannot be adequately described by the Randles circuit; but if an additional resistance is added in parallel (R_x in Fig. 1) then the spectra can be fit well (Janek et al., 1998).

Duplex DNA also contains a stacked π-system and the conductivity of native DNA (B-DNA) has been hotly debated. Recent direct measurements suggest that B-DNA is a semiconductor with a wide band gap (Storm et al., 2001; Rakitin et al., 2001; Porath et al., 2000; Murphy et al., 1993). On the other hand, oxidative cleavage events resulting from electron transfer from guanine to excited chromophores has been observed in duplexes as long as 200 Å (Henderson et al., 1999). Current models which describe electron transfer in DNA include a), simple hopping between the basepairs (Jortner et al., 1998; Bixon et al., 1999); b), long-range tunneling (Giese et al., 2001); and c), a phonon-assisted polaronlike hopping mechanism in which the cations surrounding the DNA play a central role (also called ion-gated transport; see Henderson et al., 1999; Barnett et al., 2001).

The conductivity of DNA can be improved by deposition of silver atoms along its length but the process is essentially

Submitted July 22, 2002, and accepted for publication January 17, 2003.

Address reprint requests to Heinz-Bernhard Kraatz, Dept. of Chemistry, University of Saskatchewan, 10 Science Pl., Saskatoon, SK, Canada S7N 5C9; or Jeremy S. Lee, Dept. of Biochemistry, University of Saskatchewan, 107 Wiggins Rd., Saskatoon, SK, Canada S7N 5E5.

0006-3495/03/05/3218/08 $2.00

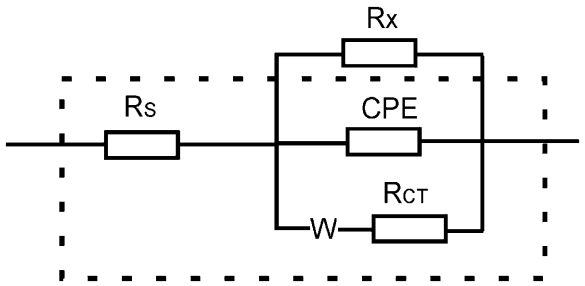

FIGURE 1 Equivalent circuit model for B-DNA and M-DNA. The circuit within the dotted box is the standard Randles circuit. R_s, solution resistance; R_x, resistance through the DNA; R_{ct}, charge transfer resistance; C, double-layer capacitance; W, Warburg impedance.

irreversible (Braun et al., 1998). Another possibility is to convert B-DNA to M-DNA by the addition of divalent metal ions (Zn^{2+}, Co^{2+}, and Ni^{2+}) at pHs above 8.5 (Lee et al., 1993; Aich et al., 1999). In M-DNA, it is proposed that the metal ions replace the amino protons of guanine and thymine in every basepair but the structure can be converted back to B-DNA by chelating the metal ions with EDTA or reducing the pH. Electron transport through M-DNA can be monitored by fluorescence spectroscopy of duplexes labeled at opposite ends with donor and acceptor chromophores. Upon formation of M-DNA the donor is quenched but only when the acceptor is on the same DNA molecule (Aich et al., 1999, 2002). Recent direct measurements have confirmed that M-DNA shows metallic-like conductivity and electron transfer can be observed in duplexes as long as 500 basepairs (Rakitin et al., 2001). Therefore, M-DNA may be useful in biosensor applications by allowing a direct electronic readout of the state of the DNA.

In this report, we have used impedance spectroscopy to study the electronic properties of B-and M-DNA self-assembled monolayers on gold electrodes. As shown in Fig. 2, upon addition of Zn^{2+} to form M-DNA the ions are inserted into the DNA helix as well as binding to the phosphate backbone outside the helix. The conversion of B- to M-DNA gives rise to characteristic changes in the impedance spectra which was observed for 15, 20, and 30 basepair duplexes. It was found that the modified Randles circuit which includes R_x, a resistance in parallel, was required to give a good fit to the experimental data (Fig. 1). In all cases M-DNA appears to decrease both R_x and R_{ct}, and promote electron transfer through the monolayer. Thus, metal ions can cause large changes in rates of electron transfer which is consistent with an ion-gated transport model (Barnett et al., 2001).

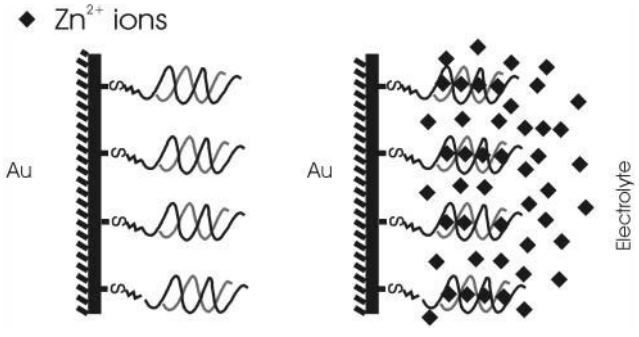

FIGURE 2 Cartoon of the native DNA (B-DNA) and metal DNA (M-DNA) on the gold electrode surface. The Zn^{2+} ions bind to the outside of the M-DNA as well as being inserted into the helix.

MATERIALS AND METHODS

Chemicals

Potassium hexaferricyanide, potassium hexaferrocyanide, hexaammineruthenium (III) chloride hexaammineruthenium (II) chloride, were from Aldrich and were ACS reagent grade. $Zn(ClO_4)_2$, $Mg(ClO_4)_2$, and Tris-ClO_4 were purchased from Fluka Co. The standard buffer was 20 mM Tris-ClO_4 at either pH 8.7 or 7.0. Other chemicals were analytical grade. All solutions were prepared in Millipore filtered water.

DNA

The probe DNAs were synthesized and purified with standard DNA synthesis methods at the Plant Biotechnology Institute, Saskatoon. The disulfide linkers were purchased from Glen Research (Sterling, VA). The oligonucleotides base sequences are: 15-mer DNA, 5′-**AAC TAC TGG GCC ATC**-$(CH_2)_3$-S-S-$(CH_2)_3$-OH-3′, target complementary sequence 5′-**GAT GGC CCA GTA GTT**-3′. 20-mer DNA, 5′-**AAC TAC TGG GCC ATC GTG AC**-$(CH_2)_3$-S-S-$(CH_2)_3$-OH-3′, target complementary sequence 5′-**GTC ACG ATG GCC CAG TAG TT**-3′, 30-mer DNA, 5′-**GTG GCT AAC TAC GCA TTC CAC GAC CAA ATG**-$(CH_2)_3$-S-S-$(CH_2)_3$-OH-3′, target complementary sequence 5′-**CAT TTG GTC GTG GAA TGC GTA GTT AGC CAC**-3′.

Electrode preparation

Gold disk electrodes (geometric surface area 0.02 cm^2) and Ag/AgCl reference electrodes were purchased from Bioanalytical Systems. Before use, the electrodes were carefully polished with a 0.05 μm alumina slurry, cleaned in 0.1M KOH solution for a few minutes, and then washed in Millipore H_2O, twice. The electrodes were carefully investigated by microscopy to ensure that there were no obvious defects. Finally, electrochemical treatment was preformed in the cell described below, by cycling from a potential of −0.1 to +1.25 V versus Ag/AgCl in 0.5M H_2SO_4 solution until a stable gold oxidation peak at 1.1 V versus Ag/AgCl was obtained (Finklea, 1996).

Preparation of DNA modified gold electrodes

DNA duplexes were prepared by adding 10 nmol of the disulphide-labeled DNA strands to 10 nmol of the complementary strands in 50 μl of 20 mM Tris-ClO_4 buffer pH 8.7 with 20 mM $NaClO_4$ for 2 h at 20°C. The final double-stranded DNA concentration is ~100 μM. The freshly prepared gold electrodes were incubated with the DNA duplexes for 5 days in a sealed container (Galka and Kraatz, 2002). The electrodes were rinsed thoroughly with buffer solution (20 mM Tris-ClO_4 and 20 mM $NaClO_4$) and mounted into an electrochemical cell. B-DNA was converted to M-DNA by the addition of 0.4 mM $Zn(ClO_4)_2$ for 2 h at pH 8.7.

X-ray photoelectron spectroscopy

A Leybold MAX200 photoelectron spectrometer equipped with an Al-Kα radiation source (1486.6 eV) was used to collect photoemission spectra at the University of Heidelberg, Germany. The base pressure during measurements was maintained at less than 10^{-9} mbar in the analysis chamber. The takeoff angle was 60°. The routine instrument calibration standard was the Au $4f_{7/2}$ peak (binding energy 84.0 eV).

Electrochemistry

A conventional three-electrode cell was used. All experiments were conducted at room temperature. The cell was enclosed in a grounded Faraday cage. The reference electrode was always isolated from the cell by a Luggin capillary containing the electrolyte. The salt-bridge reference electrode was used because of limiting Cl^- ion leakage for the normal Ag/AgCl reference electrode to the measurement system. The counter electrode was a platinum wire. Impedance spectroscopy was measured with a 1025 frequency response analyzer interfaced to an EG&G 283 potentiostat/galvanostat via GPIB on a PC running Power Suite (Princeton Applied Research). Impedance was measured at the potential of 250 mV versus Ag/AgCl, and was superimposed on a sinusoidal potential modulation of ±5 mV. The frequencies used for impedance measurements can range from 100 kHz to 100 mHz. The impedance data for the bare gold electrode, B-DNA and M-DNA modified gold electrode were analyzed using the ZSimpWin software (Princeton Applied Research). From repeated measurements, the error in R_x and R_{ct} is estimated to be ±50 Ω. In all impedance spectra, symbols represent the experimental raw data, and the solid lines are the fitted curves.

RESULTS

Assembly of the monolayer

Native duplex B-DNA was assembled on the gold surface as described in Materials and Methods. The single-stranded sequences were designed so as to contain ~50% A or T bases and to be unable to form stable alternative structures. The monolayer was characterized by cyclic voltammetry with 4 mM $K_3[Fe(CN)_6]/K_4[Fe(CN)_6]$ (1:1) mixture, as a redox probe. A typical scan is shown in Fig. 3; the bare gold electrode shows a characteristic quasi-reversible redox cycle with a peak separation of 158 mV. For the 20 basepair duplex assembled on the electrode, the peak current drops by over 95% and the separation between the oxidation and reduction peaks is increased indicating the presence of the DNA on the electrode and a reduced ability for electron transfer between the solution and the surface.

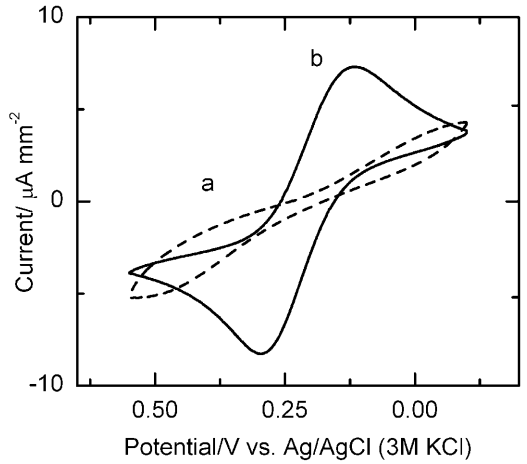

FIGURE 3 Cyclic voltammograms for (*a*) bare gold and (*b*) 20 basepair duplex B-DNA assembled on gold electrode in 4 mM $K_3[Fe(CN)_6]/K_4[Fe(CN)_6]$ (1:1), 20 mM $NaClO_4$ and 20 mM Tris-ClO_4 buffer solution (pH 8.6). Scan rate, 50 mV/s.

The gold surface was also analyzed by x-ray photoelectron spectroscopy (XPS). As shown in Fig. 4, the intensity of the Au_{4f} peaks decreases upon attachment of the DNA (either B- or M-DNA) as expected for a modified surface (Kondo et al., 1998; Ishida et al., 1999). The S_{2p} (162.4 eV), P_{2p} (133 eV), and N_{1s} (400 eV) peaks are evident in the spectra of B- and M-DNA but are not present in the spectrum of the bare gold providing good evidence for the attachment of a disulphide-linked DNA to the surface. Of particular interest is the observation that that the N_{1s} and O_{1s} spectra for B- and M-DNA (after addition of Zn^{2+} at pH 8.7) are different. This is consistent with the zinc ions interacting with the DNA double helix and more specifically with the nitrogen and oxygen atoms of the basepairs (Lee et al., 1993; Aich et al., 1999). Direct evidence for the incorporation of Zn^{2+} could not be obtained by XPS since the Zn signal lies outside the detection range of the instrument.

Impedance spectroscopy for B-DNA

Impedance measurements were performed in the presence of 4 mM $K_3[Fe(CN)_6]/K_4[Fe(CN)_6]$ (1:1) mixture, as the redox probe. Fig. 5 *A* shows a Nyquist plot for the bare gold electrode which can be described as a semicircle near the origin at high frequencies followed by a linear tail with a slope of unity. Others have described similar curves and the data can be fit adequately by the Randles circuit of Fig. 1. The diameter of the semicircle is a measure of the charge transfer resistance, R_{ct}. For the 20-mer B-DNA (Fig. 5 *B*), R_{ct} increases considerably compared to the bare electrode since electron transfer to the electrode is reduced. However, the low frequency region is no longer linear and cannot be fit adequately by a simple Randles circuit. Impedance measurements of B-DNA (and M-DNA, see below) in the absence of a redox probe (Fig. 6) demonstrated nonlinear behavior which is not expected for a simple insulator. However, the curves of Fig. 6 could be fit with a simple circuit consisting of a capacitor with a resistance in parallel. This result suggests the presence of an additional interfacial resistance, R_x, which can be added in parallel to the Randles circuit (Fig. 1). As shown in Fig. 5 *B*, the modified circuit gives an excellent fit to the experimental data in both the low and high frequency zones.

Formation of M-DNA

Upon addition of Zn^{2+} to the 20-mer B-DNA modified gold

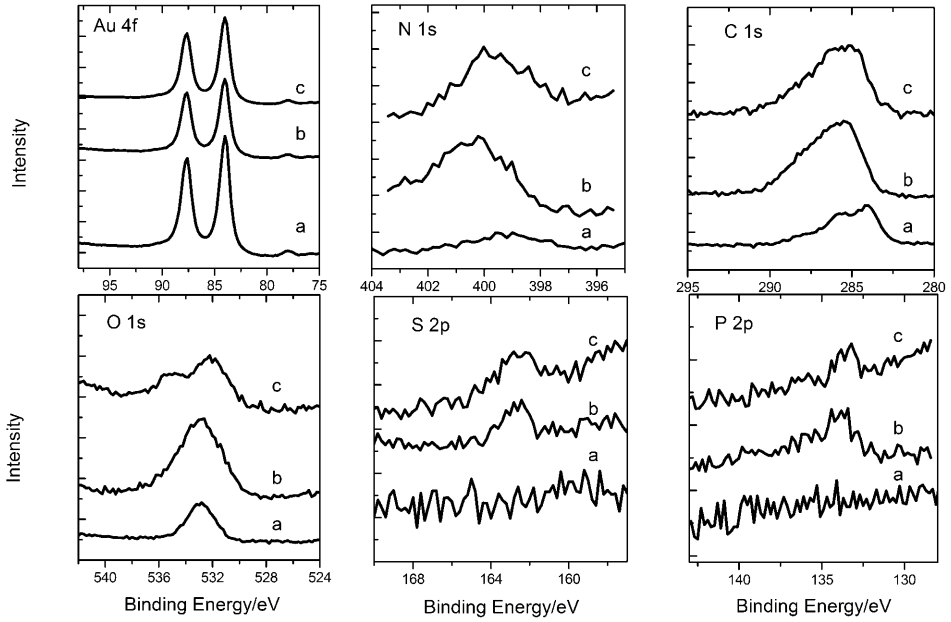

FIGURE 4 XPS spectra of (*a*) bare gold, (*b*) 20 basepair duplex B-DNA assembled on gold, and (*c*) 20 basepair duplex M-DNA assembled on gold.

electrode at pH 8.7 to form M-DNA, the impedance spectrum changed in a distinctive pattern with a reduction in Z_{im} and Z_{re} at both high and low frequencies (Fig. 5 *C*). Control experiments demonstrated that M-DNA formation was complete within 2 h. Again only the modified Randles circuit gives a good fit to the experimental data. Also shown in Fig. 5 *D* are impedance spectra for the DNA modified electrode in a pH 7.0 buffer with and without Zn^{2+} and at pH 8.7 with Mg^{2+}. Under these conditions, M-DNA does not form and only small changes in the impedance spectra are observed. The calculated values for R_s, R_x, R_{ct}, C, and W are listed in Table 1. It is clear that there are significant decreases in R_x and R_{ct} upon formation of M-DNA which are not found upon addition of Mg^{2+} nor upon addition of Zn^{2+} at pH 7.0.

DNA sequence length

To provide further information concerning the elements in the suggested model, DNA duplexes of 15, 20, and 30 basepairs were used to modify the surface of the gold electrode.

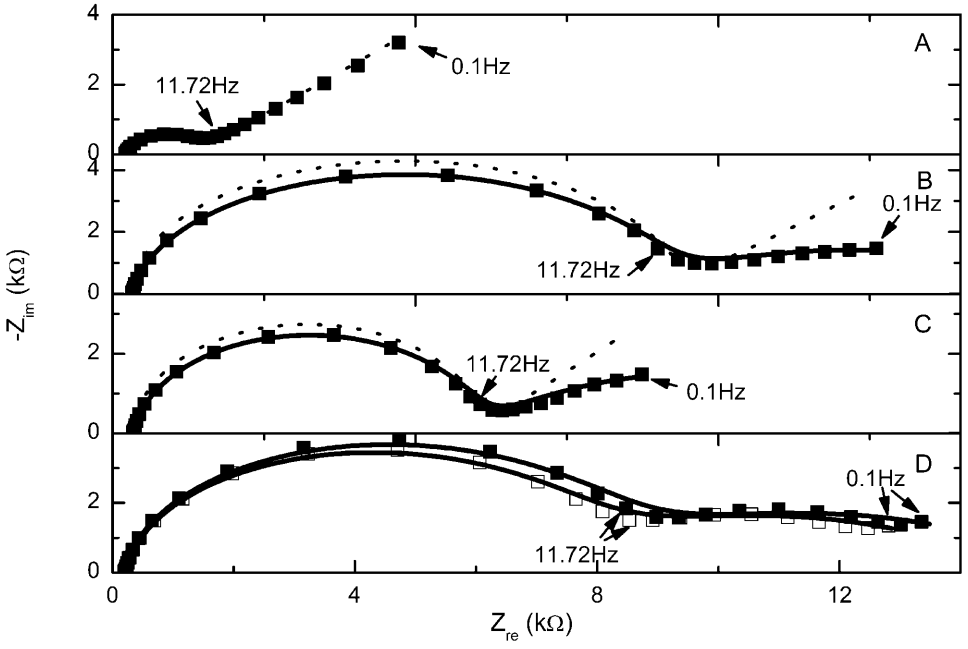

FIGURE 5 Nyquist plots (Z_{im} versus Z_{re}) with 4 mM $Fe(CN)_6^{3-/4-}$ (1:1) mixture as redox probe 20 mM Tris-ClO_4 and 20 mM $NaClO_4$ solution, applied potential 0.250 V versus Ag/AgCl. In all cases the measured data points are shown as ■ with the calculated fit to the Randles circuit as - - - - - or modified Randles circuit as ——. (*A*) Bare gold electrode, (*B*) 20 basepair duplex B-DNA assembled on gold electrode, (*C*) 20 basepair duplex M-DNA assembled on gold electrode, and (*D*) 20 basepair duplex B-DNA assembled on gold electrode with 0.4 mM Zn^{2+} at pH 7.0 (■) or with 0.4 mM Mg^{2+} at pH 8.6 (□).

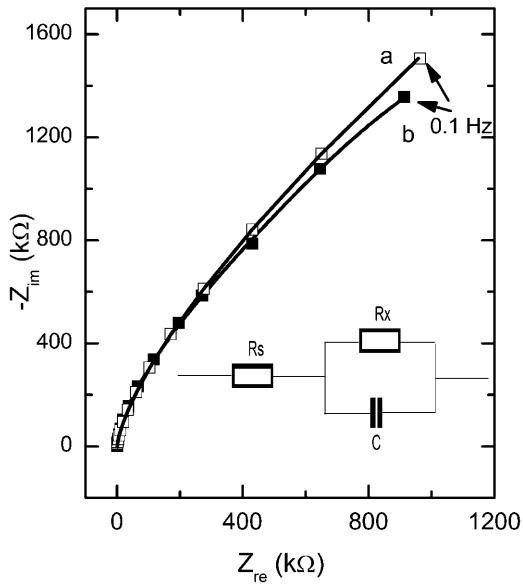

FIGURE 6 Nyquist plots in the absence of a redox probe for (*a*) 20 basepair duplex B-DNA assembled on gold (□) and (*b*) 20 basepair duplex M-DNA assembled on gold (■). The experimental data were fit to the equivalent circuit shown.

As shown in Fig. 7, all of the impedance spectra have the same characteristic shape and a fit to the modified Randles circuit is excellent. The calculated values for R_s, R_x, R_{ct}, C, and W are listed in Table 2. There are two distinct trends. First, R_x and R_{ct} increase with increasing length for both B- and M-DNA. Second, for any length of duplex R_x and R_{ct} for M-DNA is less than the corresponding value for B-DNA. W, the Warburg impedance which represents mass transfer to the electrode is more variable but in all cases is higher for the M-DNA duplexes. As expected, R_s, the solution resistance, is independent of duplex length; and C, the double layer capacitance, decreases with increasing length of the duplex.

$Ru(NH_3)_6^{3+/2+}$ redox probe

The redox probe in the above experiments was $Fe(CN)_6^{3-/4-}$ which is negatively charged and, therefore, will be repelled by the phosphodiester backbone of the DNA. $Ru(NH_3)_6^{3+/2+}$, on the other hand, is expected to be able to penetrate the monolayer. Impedance spectroscopy was performed with $Ru(NH_3)_6^{3+/2+}$ as a redox probe for the 20 basepair B- and M-DNA duplexes (Fig. 8). As shown in the inset, R_{ct} is now very small and there is very little difference between the spectra for B-DNA and M-DNA.

DISCUSSION

DNA monolayers were assembled on a gold surface and assessed by CV and XPS. The CV spectra provide good evidence for a densely-packed monolayer with good blocking against $Fe(CN)_6^{3-/4-}$, From the XPS, the film thickness was estimated based on the exponential attenuation of the Au 4*f* signal and calculated to be 45 Å. (Pressprich et al., 1989). A 20 basepair duplex is expected to have a length of ~70 Å so a measured thickness of 45 Å is consistent with the DNA protruding from the surface at an angle of ~50°. This calculation assumes that the DNA films do not collapse when the water is removed under vacuum. In general, duplex DNA attaches through the linker as compared to single-stranded DNA which can also attach through the bases (Herne and Tarlov, 1997). The value of 162.4 eV for the S_{2p} peak is also in good agreement with previous reports for alkylthiols, indicating that the DNA is interacting with the surface through an S-Au bond (Ishida et al., 1999).

AC impedance spectroscopy is an efficient method to probe and model the interfacial characterization of electrodes (Bard and Faulkner, 2001). We have chosen to present the data as Nyquist plots (Z_{im} versus Z_{re}) since characteristic changes are readily observed and interpreted. The complex impedance is presented as the sum of the real, Z_{re} (ω), and the imaginary, Z_{im} (ω) components that originate mainly from the resistance and capacitance of the measured electrochemical system, respectively. The Nyquist plot for a bare electrode is a semicircle region lying on the Z_{re} axis followed by a straight line. The semicircle portion, measured at higher frequencies, corresponds to direct electron transfer limited process, whereas the straight linear portion, observed at lower frequencies, represents the diffusion-controlled electron transfer process. The modification of the metallic surface with an organic layer decreases the double layer capacitance and retards the interfacial electron transfer rates compared to a bare metal electrode (Finklea et al., 1993a; Kharitonov et al., 2000).

For many uncharged monolayers, different redox probes give qualitatively similar results since the interaction be-

TABLE 1 Impedance values with pH and ion type

Element	Bare gold	B-DNA pH 8.6	M-DNA pH 8.6	B-DNA pH 7.0	DNA with Zn pH 7.0	DNA with Mg pH 8.6
R_s/Ω	302	320	338	327	313	334
R_x/Ω		16160	12850	15560	14650	14880
$C/\mu F$	2.6	0.288	0.285	0.289	0.318	0.355
R_{CT}/Ω	1229	18830	10009	16180	15010	15360
$W/10^{-5}\ \Omega s^{-1/2}$	27	3.9	8.2	1.9	1.8	2.0

Values derived from the modified Randles circuit except for the bare Au electrode for which the data were fit to the unmodified Randles circuit.

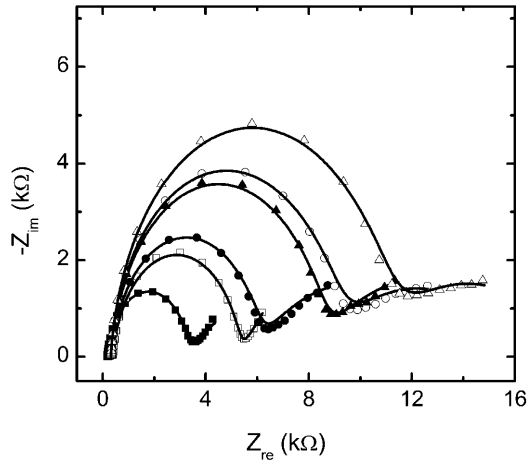

FIGURE 7 Nyquist plots with $Fe(CN)_6^{3-/4-}$ as redox probe for 15 basepair duplex monolayers as B-DNA (□) or M-DNA (■), 20 basepair duplex monolayers as B-DNA (○) or M-DNA (●), and 30 basepair duplex monolayers as B-DNA (△) or M-DNA (▲). The data points were fit to the modified Randles circuit as described in the text.

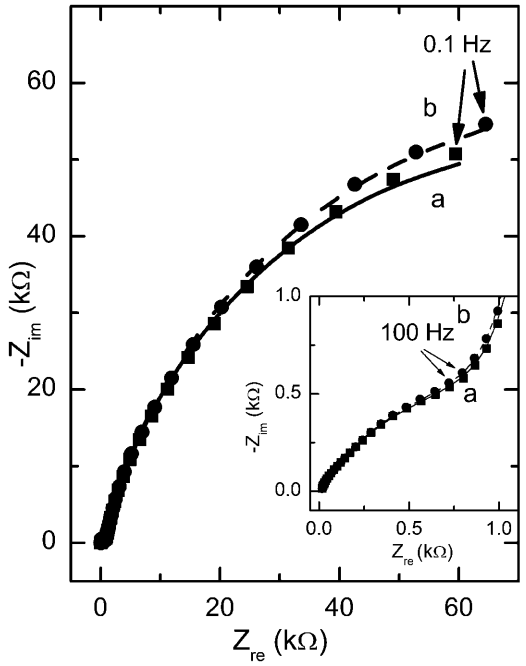

FIGURE 8 Nyquist plot for the Impedance measurements for B-DNA and M-DNA modified gold electrode in 5 mM $Ru(NH_3)^{3+/2+}$, 20 mM Tris-ClO_4 buffer solution (pH, 8.6), and applied potential −0.10 V vs. Ag/AgCl.

tween the probe and the monolayer is not electrostatic (Boubour and Lennox, 2000; Finklea, 1996; Finklea et al., 1993a). DNA, however, is negatively charged, and therefore, positively-charged probes such as $Ru(NH_3)_6^{3+/2+}$ can interact with the monolayer, whereas negatively-charged probes such as $Fe(CN)_6^{3-/4-}$ will not. These differences are clearly reflected in our results where R_{ct} with $Ru(NH_3)_6^{3+/2+}$ is ~1 kΩ (Fig. 8), similar to that of a bare electrode, whereas with $Fe(CN)_6^{3-/4-}$ and B-DNA the corresponding value is nearly 20 kΩ. Therefore, $Ru(NH_3)_6^{3+/2+}$ is not a suitable probe for impedance spectroscopy of DNA since the charge transfer can essentially bypass the monolayer.

Data analysis requires modeling the electrode kinetics with an equivalent circuit consisting of electrical components. For many monolayers the commonly accepted equivalent circuit is based on the Randles model, as shown in Fig. 1. However, to obtain a good fit to the experiment data, a parallel interfacial resistance R_x had to be added to the equivalent circuit corresponding to electron transfer through the DNA. Evidence for a parallel interfacial resistance was obtained from impedance measurements without the $Fe(CN)_6^{3-/4-}$, redox-active probe (Fig. 6). In a previous report (Yan and Sadik, 2001a,b), impedance data of DNA on a gold surface was successfully modeled with an unmodified Randles circuit. However, in this case the DNA was nearly 3000 base-pairs in length and was attached to the gold through an avidin/biotin linkage. Therefore, the electronic properties are expected to be very different.

Whereas the impedance of alkylthiol monolayers can be adequately described by the Randles model, monolayers composed of the biphenyl, HMB, cannot (Janek et al., 1998). For HMB, as with DNA, an additional parallel resistance must be included and it was suggested that this effect was due to electron transfer through the π-system of the biphenyl. The observation of electron transfer through the DNA would agree with the current views of DNA conductivity (Storm et al., 2001; Boon et al., 2000; Rakitin et al., 2001), although it is difficult to distinguish between the physical meaning of R_{ct} and R_x. Perhaps the simplest interpretation is that R_{ct} corresponds to direct electron transfer which dominates at higher frequencies, whereas R_x represents the diffusion-controlled electron transfer process which dominates at lower frequencies.

Our results also confirm that M-DNA is a better conductor than B-DNA since both R_{ct} and R_x are smaller for M-DNA.

TABLE 2 Impedance values for different length sequences

Element	15-mer B-DNA	15-mer M-DNA	20-mer B-DNA	20-mer M-DNA	30-mer B-DNA	30-mer M-DNA
R_s/Ω	322	334	320	338	319	330
R_x/Ω	12500	7681	16160	12850	17630	15760
$C/\mu F$	0.679	0.621	0.288	0.285	0.291	0.271
R_{CT}/Ω	7936	5326	18830	10009	26370	16720
$W/10^{-5}\ \Omega s^{-1/2}$	2.7	3.2	3.9	8.2	2.3	5.5

There are also small but significant increases in conductivity upon addition of Zn or Mg ions under conditions which do not allow the formation of M-DNA (Table 1). The difference between R_{ct} for B- and M-DNA tends to increase with increasing length whereas the difference in R_x decreases with increasing length of the DNA duplex. The relationship between resistance and rate of electron transfer, k_{et}, is complex, inasmuch as the DNA is not attached directly to the electrode, so that R_x and R_{ct} both contain terms in series for electron transfer from the DNA through the linker to the electrode. Nevertheless, resistance is inversely proportional to k_{et} so that the effects of duplex length and presence of metal ions do provide some insight into the mechanism of electron transfer (Finklea et al., 1993b; Pardo-Yissar et al., 2001). If electron transfer involves tunneling then k_{et} is expected to decrease exponentially with duplex length (Giese et al., 2001). Therefore, the very shallow distance dependence of resistance for both B- and M-DNA suggests that electron transfer is occurring by a hopping mechanism for which a shallow algebraic distance dependence is expected (Bixon et al., 1999). Furthermore, the effect of metal ions is consistent with the ion-gated hopping model (Barnett et al., 2001). From this perspective, the metal ions in M-DNA are very effective in promoting electron transfer because they are intimately involved in the stacking interactions of the basepairs compared to metal ions which are bound to the phosphate backbone.

The authors thank Dr. Herrwerth, the University of Heidelberg, Germany, for performing the XPS measurements.

The authors also thank the Canadian Institutes of Health Research, National Science and Engineering Research Council of Canada, and University Medical Discoveries, Inc., for financial support; H-B.K. holds a Canadian Research Chair in Biomaterials and J.S.L. is supported by a Senior Investigator Award from the Regional Partnership Program of the Canadian Institutes of Health Research. Y-T.L. was supported by a Health Services Utilization and Research Commission postdoctoral fellowship.

REFERENCES

Aich, P., L. Labiuk, W. Tari, L. J. T. Delbaere, W. J. Roesler, K. J. Falk, R. P. Steer, and J. S. Lee. 1999. M-DNA: a complex between divalent metal ions and DNA which behaves as a molecular wire. *J. Mol. Biol.* 294: 477–483.

Aich, P., R. J. S. Skinner, S. D. Wettig, R. P. Steer, and J. S. Lee. 2002. Long range molecular wire behaviour in a metal complex of DNA. *J. Biomol. Struct. Dyn.* 20:1–6.

Alfonta, L., and I. Willner. 2001. Electronic transduction of biocatalytic transformations on nucleic acid-functionalized surfaces. *Chem. Commun.* 1492–1493.

Ambroise, A., and B. G. Maiya. 2000. Ruthenium(II) complexes of redox-related, modified dipyridophenazine ligands: synthesis, characterization, and DNA interaction. *Inorg. Chem.* 39:4256–4263.

Bard, A. J., and L. R. Faulkner. 2001. Electrochemical Methods: Fundamentals and Applications. John Wiley & Sons, Inc., New York.

Bardea, A., F. Patolsky, A. Dagan, and I. Willner. 1999. Sensing and amplification of oligonucleotide-DNA interactions by means of impedance spectroscopy: a route to a Tay-Sachs sensor. *Chem. Commun.* 21–22.

Barnett, R. N., C. L. Cleveland, A. Joy, U. Landman, and G. B. Schuster. 2001. Charge migration in DNA: ion-gated transport. *Science.* 294:567–571.

Bixon, M., B. Giese, S. Wessely, T. Langenbacher, M. E. Michel-Beyerle, and J. Jortner. 1999. Long-range charge hopping in DNA. *Proc. Natl. Acad. Sci. USA.* 96:11713–11716.

Boon, E. M., D. M. Ceres, T. G. Drummond, M. G. Hill, and J. K. Barton. 2000. Mutation detection by electrocatalysis at DNA-modified electrodes. *Nat. Biotechnol.* 18:1096–1100.

Boubour, E., and R. B. Lennox. 2000. Insulating properties of self-assembled monolayers monitored by impedance spectroscopy. *Langmuir.* 16:4222–4228.

Braun, E., Y. Eichen, U. Sivan, and G. Ben Yoseph. 1998. DNA-templated assembly and electrode attachment of a conducting silver wire. *Nature.* 391:775–778.

Carter, M. T., and A. J. Bard. 1987. Voltammetric studies of the interaction of tris(1,10-phenanthroline)cobalt(III) with DNA. *J. Am. Chem. Soc.* 109:7528–7530.

Colonna, B., and L. Echegoyen. 2001. Templated SAMs for metal recognition. *Chem. Commun.* 1104–1105.

Finklea, H. O., D. A. Snider, J. Fedyk, E. Sabatani, Y. Gafni, and I. Rubinstein. 1993a. Characterization of octadecanethiol-coated gold electrodes as microarray electrodes by cyclic voltammetry and AC impedance spectroscopy. *Langmuir.* 9:3660–3667.

Finklea, H. O., M. S. Ravenscroft, and D. A. Snider. 1993b. Electrolyte and temperature effects on long range electron transfer across self-assembled monolayers. *Langmuir.* 9:223–227.

Finklea, H. O. 1996. Electroanalytical Chemistry. Marcel Dekker Inc., New York.

Fodor, S. P. A., R. P. Rava, X. H. C. Huang, A. C. Pease, and C. P. Holmes. 1993. Multiplexed biochemical assays with biological chips. *Nature.* 364:555–556.

Giese, B., J. Amaudrut, A. K. Kohler, M. Spormann, and S. Wessely. 2001. Direct observation of hole transport between adenine bases and by tunnelling. *Nature.* 412:318–320.

Gooding, J. J. 2002. Electrochemical DNA hybridization biosensors. *Electroanalysis.* 14:1149–1156.

Galka, M. M., and H.-B. Kraatz. 2002. Electron transfer studies on self-assembled monolayers of helical ferrocenoyl-oligoproline-cystamine bound to gold. *Chem. Phys. Chem.* 3:356–359.

Hashimoto, K., K. Ito, and Y. Ishimori. 1994. Sequence-specific gene detection with a gold electrode modified with DNA probes and an electrochemically active dye. *Anal. Chem.* 66:3830–3833.

Henderson, P. T., D. Jones, G. Hampikian, Y. Kan, and G. B. Schuster. 1999. Long-distance charge transport in duplex DNA: the phonon assisted polaron-like hopping mechanism. *Proc. Natl. Acad. Sci. USA.* 96:8353–8358.

Herne, T. M., and M. J. Tarlov. 1997. Characterization of DNA probes immobilized on gold surface. *J. Am. Chem. Soc.* 119:8916–8920.

Ishida, T., N. Choi, W. Mizutani, H. Tokumoto, I. Kojima, H. Azehara, H. Hokari, U. Akiba, and M. Fujihira. 1999. High-resolution x-ray photoelectron spectra of organosulfur monolayers on Au(111): S(2p) spectral dependence on molecular species. *Langmuir.* 15:6799–6806.

Jackson, N. M., and M. G. Hill. 2001. Electrochemistry at DNA-modified surfaces: new probes for charge transport through the double helix. *Curr. Opin. Chem. Biol.* 5:209–215.

Janek, R. P., W. R. Fawcett, and A. Ulman. 1998. Impedance spectroscopy of self-assembled monolayers on Au(111): sodium ferrocyanide charge transfer at modified electrodes. *Langmuir.* 14:3011–3018.

Jortner, J., M. Bixon, T. Langenbacher, and M. E. Michel-Beyerle. 1998. Charge transfer and transport in DNA. *Proc. Natl. Acad. Sci. USA.* 95:12759–12765.

Kelley, S. O., J. K. Barton, N. M. Jackson, and M. G. Hill. 1997. Electrochemistry of methylene blue bound to a DNA-modified electrode. *Bioconjugate Chem.* 8:31–37.

Kelly, S. O., N. M. Jackson, M. G. Hill, and J. K. Barton. 1999. Long-range electron transfer through DNA films. *Angew. Chem. Int. Ed.* 38: 941–945.

Kertesz, V., N. A. Whittemore, J. Q. Chambers, M. S. McKinney, and D. C. Baker. 2000. Surface titration of DNA-modified gold electrodes with a thiol-tethered anthraquinone. *J. Electroanal. Chem.* 493:28–36.

Kharitonov, A. B., L. Alfonta, E. Katz, and I. Willner. 2000. Probing of bioaffinity interactions at interfaces using impedance spectroscopy and chronopotentiometry. *J. Electroanal. Chem.* 487:133–141.

Kim, K., and J. Kwak. 2001. Faradaic impedance titration of pure 3-mercaptopropionic acid and ethanethiol mixed monolayers on gold. *J. Electroanal. Chem.* 512:83–91.

Kondo, T., M. Yanagida, K. Shimazu, and K. Uosaki. 1998. Determination of thickness of a self-assembled monolayer of dodecanethiol on Au(111) by angle-resolved z-ray photoelectron spectroscopy. *Langmuir*. 14:5656–5658.

Lee, J. S., L. J. P. Latimer, and R. S. Reid. 1993. A cooperative conformational change in duplex DNA induced by Zn^{2+} and other divalent metal ions. *Biochem. Cell Biol.* 71:162–168.

Lee, T.-Y., and Y.-B. Shim. 2001. Direct DNA hybridization detection based on the oligonucleotide-functionalized conductive polymer. *Anal. Chem.* 73:5629–5632.

Macdonald, J. R. 1987. Impedance Spectroscopy. John Wiley & Sons, New York.

Millan, K. M., A. Saraullo, and S. R. Mikkelsen. 1994. Diagnosis of cystic fibrosis in PCR-amplified human DNA using voltammetric DNA sensors. *Anal. Chem.* 66:2943–2948.

Murphy, C. J., M. R. Arkin, Y. Enkins, N. D. Ghatlia, S. H. Bossmann, N. J. Turro, and J. K. Barton. 1993. Long-range photoinduced electron-transfer through a DNA helix. *Science.* 262:1025–1029.

Patolsky, F., A. Lichtenstein, and I. Willner. 2001. Electronic transduction of DNA sensing processes on surfaces: amplification of DNA detection and analysis of single-base mismatches by tagged liposomes. *J. Am. Chem. Soc.* 123:5194–5205.

Pardo-Yissar, V., E. Katz, O. Lioubashevski, and I. Willner. 2001. Layered polyelectrolyte films on Au electrodes. *Langmuir*. 17:1110–1118.

Porath, D., A. Bezryadin, S. de Vries, and C. Dekker. 2000. Direct measurement of electrical transport through DNA molecules. *Nature*. 403: 635–638.

Pressprich, K. A., S. G. Maybury, R. E. Thomas, R. W. Linton, E. A. Irene, and R. W. Murray. 1989. Molecular sieving by electropolymerized porphyrin films only a few monolayers thick. *J. Phys. Chem.* 93:5568–5574.

Rakitin, A., P. Aich, C. Papaopoulos, Y. Kobzar, A. S. Vedeneev, J. S. Lee, and J. M. Xu. 2001. Metallic conduction through engineered DNA: DNA nanoelectronic building blocks. *Phys. Rev. Lett.* 86:3670–3673.

Randles, J. E. B. 1947. Kinetics of rapid electrode reactions. *Discuss. Faraday Soc.* 1:11–19.

Schena, M., D. Shalon, R. Heller, A. Chai, P. O. Brown, and R. W. Davis. 1996. Parallel human genome analysis: microarray-based expression monitoring of 1000 genes. *Proc. Natl. Acad. Sci. USA*. 93:10614–10619.

Storm, A. J., J. van Noort, S. de Vries, and C. Dekker. 2001. Insulating behavior for DNA molecules between nanoelectrodes at the 100 nm length scale. *Appl. Phys. Lett.* 79:3881–3883.

Takagi, M. 2001. Threading intercalation to double-stranded DNA and the application to DNA sensing. Electrochemistry array technique. *Pure Appl. Chem.* 73:1573–1577.

Tani, A., A. J. Thomson, and J. N. Butt. 2001. Methylene blue as an electrochemical discriminator of single- and double-stranded oligonucleotides immobilised on gold substrates. *Analyst.* 126:1756–1759.

Ulman, A. 1996. Formation and structure of self-assembled monolayers. *Chem. Rev.* 96:1533–1554.

Yan, F., and O. A. Sadik. 2001a. Enzyme-modulated cleavage of dsDNA for studying interfacial biomolecular interactions. *J. Am. Chem. Soc.* 123:11335–11340.

Yan, F., and O. A. Sadik. 2001b. Enzyme-modulated cleavage of dsDNA for supramolecular design of biosensors. *Anal. Chem.* 73:5272–5280.